Asociación Argentina
de Mecánica Computacional

Mecánica Computacional Vol XXVII, págs. 1519-1530 (artículo completo)
Alberto Cardona, Mario Storti, Carlos Zuppa. (Eds.)
San Luis, Argentina, 10-13 Noviembre 2008

SEMI-ANALYTICAL SOLUTION OF THE THERMAL FIELD INDUCED BY A MOVING DOUBLE-ELLIPSOIDAL WELDING HEAT SOURCE IN A SEMI-INFINITE BODY

Víctor D. Fachinotti and Alberto Cardona

Centro Internacional de Métodos Computacionales en Ingeniería (CIMEC-INTEC) – Universidad Nacional del Litoral (UNL) / Consejo Nacional de Investigaciones Científicas y Técnicas (CONICET)
Güemes 3450, S3000GLN Santa Fe, Argentina – E-mails: vfachino@intec.unl.edu.ar, acardona@intec.unl.edu.ar, http://www.intec.unl.edu.ar

Keywords: double-ellipsoidal heat source, welding, analytical solution, finite element method.

Abstract. This paper introduces the solution of the thermal field induced in a semi-infinite body by a moving heat source with Gaussian distribution inside a double-ellipsoidal volume. This heat source model was introduced by Goldak et al. (1984) for the simulation of welding processes. It is the most widely used model nowadays mainly thanks to its versatility to accommodate a wide variety of welding techniques. Two different semi-ellipsoidal volumes are defined corresponding to the front and the rear of the moving source. The analytical solution proposed by Nguyen et al. (1999) is only correct when both semi-ellipsoids are equal, i.e. for Goldak et al.'s (not-double-) ellipsoidal model. The correction needed to extend Nguyen et al.'s analytical solution to the double-ellipsoidal case is presented here.

The same problem is then solved using two- and three-dimensional finite element models, in order to evaluate these models in terms of accuracy and computational cost.

1 INTRODUCTION

The thermal analysis of a welding process implies the solution of a heat transfer problem with a highly concentrated, often mobile, heat source. The most widely used heat source model in numerical analysis of welding is the moving double-ellipsoidal model proposed by Goldak et al. (1984), which stands out for its versatility to accommodate different fusion welding techniques, including gas metal arc welding (GMAW) (Abid and Siddique, 2005; Abid et al., 2005; Gery et al., 2005; Nguyen et al., 1999, 2004), gas tungsten arc welding (GTAW) (Gery et al., 2005; Bang et al., 2002; Branza et al., 2004; Deng and Murakawa, 2006b,a; Duranton et al., 2004; Lei et al., 2006; Lundbäck et al., 2003; Thiessen et al., 2006; Wu and Yan, 2006; Wu et al., 2007), shielded metal arc welding (Bang et al., 2002), submerged arc welding (Goldak et al., 1984), laser spot welding (De et al., 2003), electron beam welding (Goldak et al., 1984; Goldschmied et al., 1990), laser-GMA hybrid welding (Reutzel et al., 2005).

Analytical solutions, although limited to particular situations, are fundamental for the validation of sophisticated numerical models. To this end, recourse is often made to experimental results as reference values (Goldak et al., 1984). The double-ellipsoidal heat source model has enough adjustable parameters to calibrate the model and force numerical results fit experiments, even when the numerical model is simplified, e.g. by using a coarse mesh or a large time step. Therefore, in order to asses the accuracy of a finite element model in terms of mesh and time step size, it is much better to compare to an analytical solution of a representative problem, free of measurement errors.

In this work, we solve analytically the problem of heat conduction induced by a Goldak's double-ellipsoidal heat source in a semi-infinite domain, as a first approach for the simulation of welding on thick plates. With the analytical solution at hand, the accuracy of 3D and 2D finite element models is finally evaluated.

2 MOVING DOUBLE-ELLIPSOIDAL HEAT SOURCE PROBLEM

Let us consider a fixed Cartesian reference frame x, y, z. A heat source located at $z = 0$ at time $t = 0$ moves with constant velocity v along the z-axis. Goldak et al. (1984) defined for welding applications the heat emitted at a point (x, y, z) at instant t by means of the double-ellipsoidal law:

$$q(x,y,z,t) = \frac{6\sqrt{3}Q}{\pi\sqrt{\pi}ab} \times \begin{cases} \frac{f_f}{c_f} \exp\left[-3\frac{x^2}{a^2} - 3\frac{y^2}{b^2} - 3\frac{(z-vt)^2}{c_f^2}\right], & \text{for } z > vt, \\ \frac{f_r}{c_r} \exp\left[-3\frac{x^2}{a^2} - 3\frac{y^2}{b^2} - 3\frac{(z-vt)^2}{c_r^2}\right], & \text{for } z < vt. \end{cases} \tag{1}$$

where Q is the energy input rate, a, b and c_r (resp. c_f) are the radii of the rear (resp. front) ellipsoid, and f_r (resp. f_f) is the portion of the heat deposited in the rear (resp. front) ellipsoid, with $f_r + f_f = 2$ (see Figure 1).

Let us note that

$$\int_{-\infty}^{\infty}\int_{-\infty}^{\infty}\int_{-\infty}^{\infty} q(x,y,z,t)\,\mathrm{d}x\,\mathrm{d}y\,\mathrm{d}z = 2Q \tag{2}$$

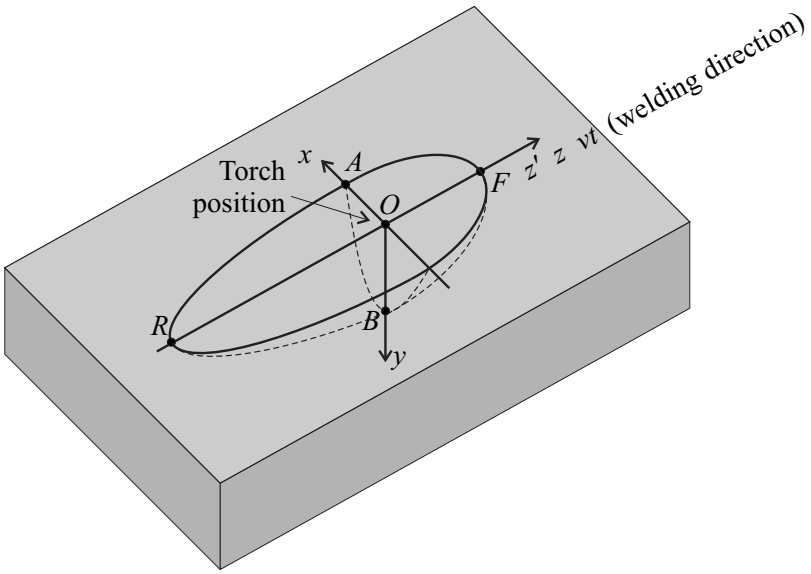

Figure 1: Double-ellipsoidal heat source model (Goldak et al., 1984).

For arc welding, the energy input rate Q can be expressed as

$$Q = \eta V I \tag{3}$$

where η is the arc efficiency, V the voltage and I the current intensity.

Calibration of the Goldak et al's double-ellipsoidal heat source model implies to adjust the six parameters η, a, b c_f, c_r and f_f in order to make analytical or numerical results fit experimental data. Some authors (Nguyen et al., 1999; Lundbäck et al., 2003; Nguyen et al., 2004) reduce the number of adjustable parameters by imposing the additional constraint $f_f/c_f = f_r/c_r$ in order to force the continuity of the function q across the plane $z = vt$ at any instant t: this yields

$$f_f = \alpha c_f/(c_r + c_f) \tag{4}$$

with $\alpha = 2$. This condition is usually ignored in the literature on welding modelling: α was found to lie between 1.8 (Goldak et al., 1984) and 3 (Goldak et al., 1984; Gery et al., 2005; Reutzel et al., 2005; Song et al., 2003), the latter matching with the choice of $c_r = 4c_f$ and $f_f = 0.6$, as suggested by Goldak et al. (1984) as default in absence of better data. Let us note that the temperature field induced by the double-ellipsoidal heat source q is always continuous, independently of the value of α.

3 INDUCED TEMPERATURE FIELD

Heat conduction in an homogeneous solid is governed by the linear partial differential equation

$$\rho c \frac{\partial T}{\partial t} - k\nabla^2 T = q \tag{5}$$

where $T = T(x, y, z, t)$ is the temperature at point (x, y, z) at time t, q the heat source, ρ the density, c the heat capacity, and k the thermal conductivity.

The fundamental solution of equation (5) is the Green function (Carslaw and Jaeger, 1959)

$$G(x-x', y-y', z-z', t-t') = \frac{1}{\rho c \left[4\kappa\pi(t-t')\right]^{3/2}} \exp\left[-\frac{(x-x')^2+(y-y')^2+(z-z')^2}{4\kappa(t-t')}\right] \quad (6)$$

where $\kappa = k/(\rho c)$ is the thermal diffusivity.

Equation (6) gives the temperature increment at point (x, y, z) and instant t due to an instantaneous unit heat source applied at point (x', y', z') at instant t', assuming the body to be infinite with an initial homogeneous temperature. Then, due to the linearity of equation (5), the temperature variation induced at point (x, y, z) at time t by an instantaneous heat source of magnitude $q(x', y', z', t')$ applied at (x', y', z') at time t' is

$$q(x', y', z', t')G(x-x', y-y', z-z', t-t') \quad (7)$$

Assuming that heat has been continuously generated at the point (x', y', z') from $t' = 0$, the temperature increment at point (x, y, z) at time t is

$$\int_0^t q(x', y', z', t')G(x-x', y-y', z-z', t-t')\,\mathrm{d}t' \quad (8)$$

If we assume that the heat has been continuously generated from $t' = 0$ throughout an infinite medium, the temperature increment at any point (x, y, z) and at any instant t takes the form

$$\Delta T(x, y, z, t) = \int_0^t \int_{-\infty}^{\infty} \int_{-\infty}^{\infty} \int_{-\infty}^{\infty} q(x', y', z', t')G(x-x', y-y', z-z', t-t')\,\mathrm{d}x'\,\mathrm{d}y'\,\mathrm{d}z'\,\mathrm{d}t' \quad (9)$$

Then, the temperature induced by the double-ellipsoidal heat source defined by equation (1) is

$$\Delta T(x, y, z, t) = \frac{3\sqrt{3}}{4\pi^3}\frac{Q}{\kappa^{3/2}ab}\int_0^t I_x I_y \left(\frac{f_r}{c_r}I_z^r + \frac{f_f}{c_f}I_z^f\right)(t-t')^{-3/2}\,\mathrm{d}t' \quad (10)$$

where

$$I_x = \int_{-\infty}^{\infty} \exp\left[-3\frac{x'^2}{a^2} - \frac{(x-x')^2}{4\kappa(t-t')}\right] \mathrm{d}x'$$
$$= 2a\sqrt{\pi}\sqrt{\frac{\kappa(t-t')}{12\kappa(t-t')+a^2}} \exp\left[-3\frac{x^2}{12\kappa(t-t')+a^2}\right] \quad (11)$$

$$I_y = \int_{-\infty}^{\infty} \exp\left[-3\frac{y'^2}{b^2} - \frac{(y-y')^2}{4\kappa(t-t')}\right] \mathrm{d}y'$$
$$= 2b\sqrt{\pi}\sqrt{\frac{\kappa(t-t')}{12\kappa(t-t')+b^2}} \exp\left[-3\frac{y^2}{12\kappa(t-t')+b^2}\right] \quad (12)$$

$$I_z^r = \int_{-\infty}^{vt'} \exp\left[-3\frac{(z'-vt')^2}{c_r^2} - \frac{(z-z')^2}{4\kappa(t-t')}\right] \mathrm{d}z'$$
$$= c_r\sqrt{\pi}\sqrt{\frac{\kappa(t-t')}{12\kappa(t-t')+c_r^2}} \exp\left[-3\frac{(z-vt')^2}{12\kappa(t-t')+c_r^2}\right]$$
$$\times \left\{1 - \mathrm{erf}\left[\frac{c_r}{2}\frac{z-vt'}{\sqrt{\kappa(t-t')}\sqrt{12\kappa(t-t')+c_r^2}}\right]\right\} \quad (13)$$

$$I_z^f = \int_{vt'}^{\infty} \exp\left[-3\frac{(z'-vt')^2}{c_f^2} - \frac{(z-z')^2}{4\kappa(t-t')}\right] \mathrm{d}z'$$
$$= c_f\sqrt{\pi}\sqrt{\frac{\kappa(t-t')}{12\kappa(t-t')+c_f^2}} \exp\left[-3\frac{(z-vt')^2}{12\kappa(t-t')+c_f^2}\right]$$
$$\times \left\{1 + \mathrm{erf}\left[\frac{c_f}{2}\frac{z-vt'}{\sqrt{\kappa(t-t')}\sqrt{12\kappa(t-t')+c_f^2}}\right]\right\} \quad (14)$$

Finally, by assuming that the body was initially at the homogeneous temperature T_0, the temperature field is defined by

$$T(x,y,z,t) = T_0 +$$
$$\frac{3\sqrt{3}}{\pi\sqrt{\pi}} Q \int_0^t \frac{\exp\left[-3\frac{x^2}{12\kappa(t-t')+a^2} - 3\frac{y^2}{12\kappa(t-t')+b^2}\right]}{\sqrt{12\kappa(t-t')+a^2}\sqrt{12\kappa(t-t')+b^2}} \left[f_r A_r\left(1-B_r\right) + f_f A_f\left(1+B_f\right)\right] \mathrm{d}t' \quad (15)$$

with

$$A_i = A(z,t,t';c_i) = \frac{\exp\left[-3\frac{(z-vt')^2}{12\kappa(t-t')+c_i^2}\right]}{\sqrt{12\kappa(t-t')+c_i^2}} \tag{16}$$

$$B_i = B(z,t,t';c_i) = \text{erf}\left[\frac{c_i}{2}\frac{z-vt'}{\sqrt{\kappa(t-t')}\sqrt{12\kappa(t-t')+c_i^2}}\right] \tag{17}$$

The time integral in equation (15) does not have a closed analytical expression, and recourse must be made to numerical integration. To this end, we use recursive adaptive Simpson quadrature, approximating the integral to within an absolute error tolerance of 10^{-6}.

Remark I: In the solution proposed by Nguyen et al. (1999) for the same problem, the terms involving B_i are lacking, making their solution valid only when $c_r = c_f$ and $f_r = f_f = 1$.

Remark II: By considering the symmetry of the solution (15) with respect to the plane $y = 0$, this solution can also be interpreted as the increment of temperature induced by q in the semi-infinite body $y \geq 0$, assuming that the surface $y = 0$ is adiabatic. This may be considered as a first approach to the problem of welding on a thick plate.

4 APPLICATION

Let us consider the problem of heat conduction in the semi-infinite domain $y \geq 0$, with the material and process data listed in Table 4. It is assumed that welding starts at point $O(0,0,0)$ at $t = 0$ and the welding torch moves with constant velocity $v = 5$ mm/s along the z-axis.

Three different cases are studied, corresponding to different choices of the parameters defining the size and the portion of heat absorbed by the front and rear semi-ellipsoids. In all cases, the fractions of the total heat corresponding to the front and the rear semi-ellipsoids are defined as

$$f_f = 2\frac{c_f}{c_f + c_r} = 2 - f_r \tag{18}$$

which forces the heat power density function q given by equation (1) to be continuous at the plane $z = vt$ at any instant t.

In Figure 2, we observe the temperature evolution at a point located along the welding axis at a distance of 5 cm from the welding start (the welding torch is directly over this point at $t = 10$ sec). Figure 3 shows the temperature along the welding axis 10 sec after the start of welding, i.e., when the welding torch is located 5 cm-far from the starting point.

As mentioned above, the error-function terms in equation (15) are missing in the solution proposed by Nguyen et al. (1999), explaining why their results are identical for cases 2 and 3, where c_f and c_r, and also f_f and f_r in virtue of equation (18), are interchanged. Nguyen et

al's solution is correct only for the case $c_f = c_r$ and $f_f = f_r$, when the error-function terms in equation (15) cancel themselves.

As it can be observed in Figures 2 and 3, the solutions proposed here reproduce the expected effect of the double-ellipsoidal heat source, with the front and rear semi-ellipsoids of different dimensions receiving different fractions of the total heat input. As shown on Figure 2, with the current solution, the increase of temperature induced by the source at a given point along the welding path is observed earlier for case 3 than for cases 1 and 2, coinciding with the fact that the front semi-ellipsoid in the welding direction for case 3 is longer than that of cases 1 and 2.

ρ	$7820\ \mathrm{kg/m^3}$		
c	$600\ \mathrm{J/(kg^oC)}$		
k	$29\ \mathrm{W/(m^oC)}$		
T_0	$20\ ^\mathrm{o}\mathrm{C}$		
v	$5\ \mathrm{mm/s}$		
Q	5083 W		
a	10 mm		
b	2 mm		
Case	1	2	3
c_f	15 mm	6 mm	24 mm
c_r	15 mm	24 mm	6 mm
f_f	1	0.4	1.6

Table 1: Moving double-ellipsoidal heat source in a semi-infinite body: material and process data.

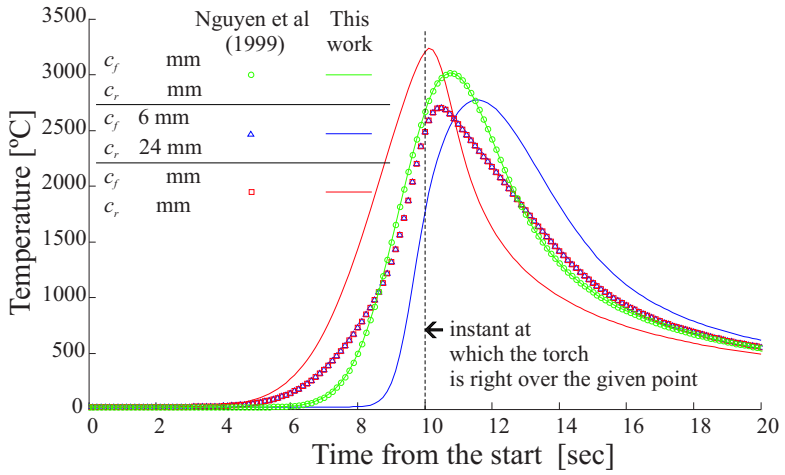

Figure 2: Analytical solutions for the temperature variation with time at the point $(0, 0, 5\ \mathrm{cm})$.

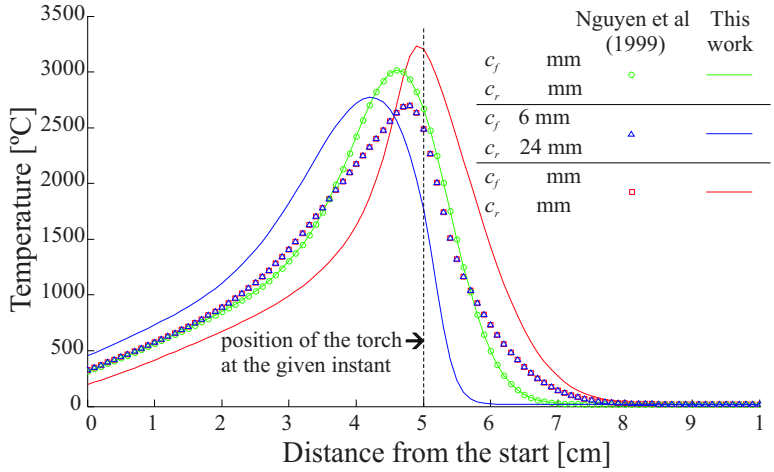

Figure 3: Analytical solutions for the temperature profile along the welding path 10 sec after the start of welding.

4.1 Validation of finite element models

With an analytical solution at hand, the accuracy of two different finite element (FEM) approximations of the solution of the heat conduction induced by a moving double-ellipsoidal heat source will be evaluated. In both cases, the fully implicit Euler-backward technique is used for time discretization. Both finite element models are implemented in the code OOFELIE (Open Engineering, 2008).

The semi-infinite medium is approximated by the thick plate $0 \leq x \leq 10$ cm (symmetry with respect to plane $x = 0$ is invoked), $0 \leq y \leq 10$ cm, -5 cm$\leq z \leq 15$ cm, as shown in Figure 4. Welding begins at point $O(0, 0, 0)$ at time $t = 0$, and follows the path $\overline{OF}$.

An unstructured mesh of 65557 linear tetrahedral elements (13547 nodes) is used to discretize the domain (see Figure 4 on the right). The mesh is gradually refined towards the welding axis, where the average element size is $h = 0.84$ mm. The time step is set to 0.05 sec, constant along the analysis.

The analytical solution also serves to assert the validity of certain simplifications that are widely accepted in numerical modelling, particularly the dimensional reduction to two dimensions, which is the most common way to reduce the computing time (Goldak et al., 1986; Goldak and Akhlaghi, 2005). The 2D models usually represent either a thin plate by a plane shell or a plane section normal to the welding direction. The latter model is well-suited for the thick plates addressed in this work. The accuracy of this model increases as the Peclet number increases (Mendez, 1995). Peclet number is proportional to welding velocity and the characteristic dimension in the welding direction, say L, and inversely proportional to the diffusivity of the material, i.e.

$$Pe = \frac{vL}{\kappa}. \tag{19}$$

By adopting $L = 10$ cm, we obtain $Pe = 80.9$, validating the use of the 2D cross-sectional model. The cross section located at $z \equiv z_{2D} = 5$ cm is chosen for the analysis. An unstructured

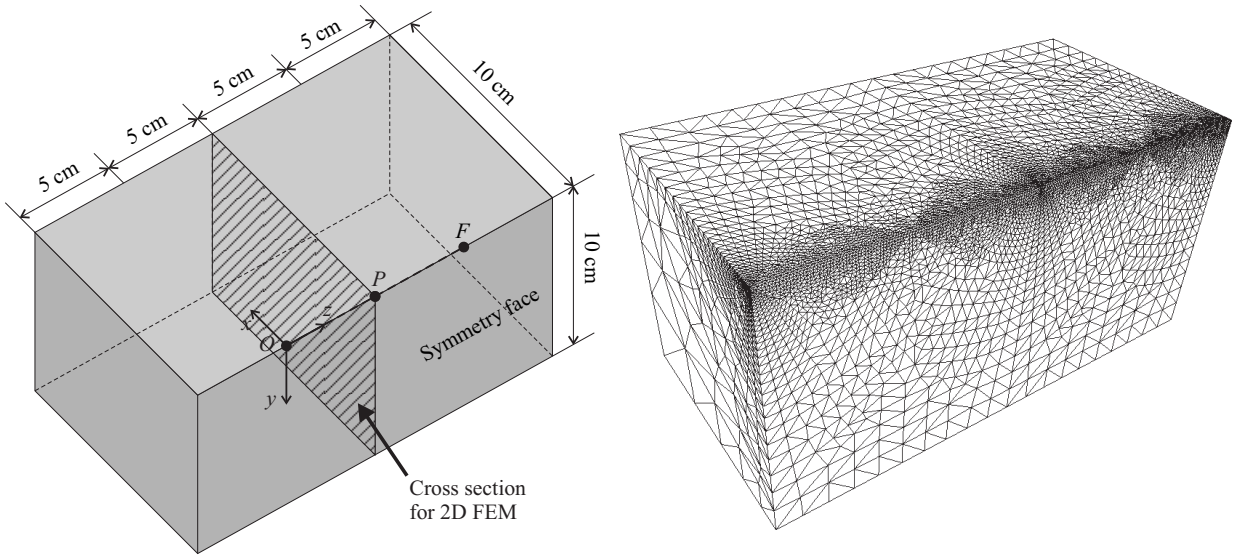

Figure 4: Finite element analysis of the temperature induced by a moving double-ellipsoidal heat source in a semi-infinite body: geometry and mesh of linear tetrahedra.

mesh of 486 linear triangular finite elements (280 nodes) is used. The mesh size is equivalent to that of the 3D mesh (in fact, the 2D mesh is the face $z = -5$ cm of the current 3D mesh). The time step is again adopted equal to 0.05 sec.

Now, taking into account that the temperature distribution is stationary with respect to a coordinate system attached to the torch moving with constant speed v along the z-axis, the 3D temperature field becomes completely determined from the 2D temperature field by using the relationship

$$T(x, y, z, t) = T(x, y, z_{2D}, t + (z_{2D} - z)/v) \tag{20}$$

Let us compare numerical and analytical results. As shown in Figures 5 and 6, the 3D FEM model fits the analytical curves with high accuracy, either for the evolution of temperature at the point P or the temperature profile along $\overline{OF}$ at $t = 10$ sec. On the other hand, the 2D FEM model gives satisfactory results for the evolution of the temperature at P (which is located at the considered cross section) for the whole time interval of interest, while the temperature predicted along $\overline{OF}$ at $t = 10$ sec agrees with the analytical solution except at the proximity of the starting point of welding. This coincides with Goldak et al's observations (Goldak et al., 1986; Goldak and Akhlaghi, 2005) on the inability of the 2D-cross sectional model to account for run-on effects.

Last but not least, there is an impressive difference regarding the CPU consumption: 5288.53 sec for the 3D FEM against 13.70 sec for the 2D FEM in a PC with Intel Core 2 Duo 6300.

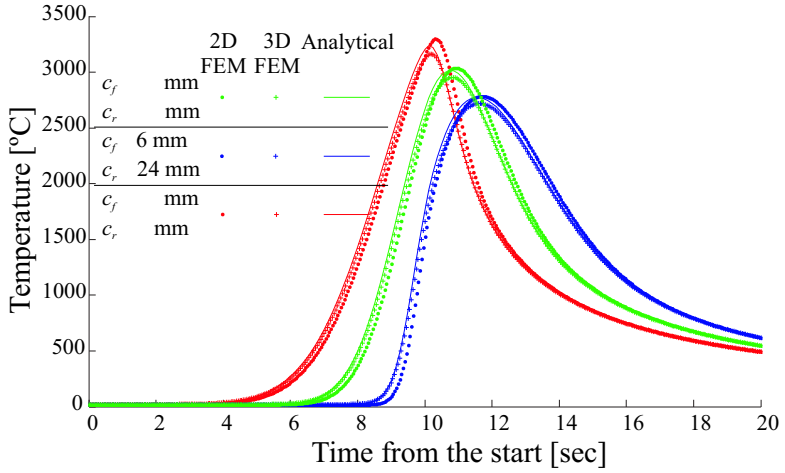

Figure 5: Analytical vs. FEM solutions for the temperature variation with time at the point $(0, 0, 5\ \text{cm})$.

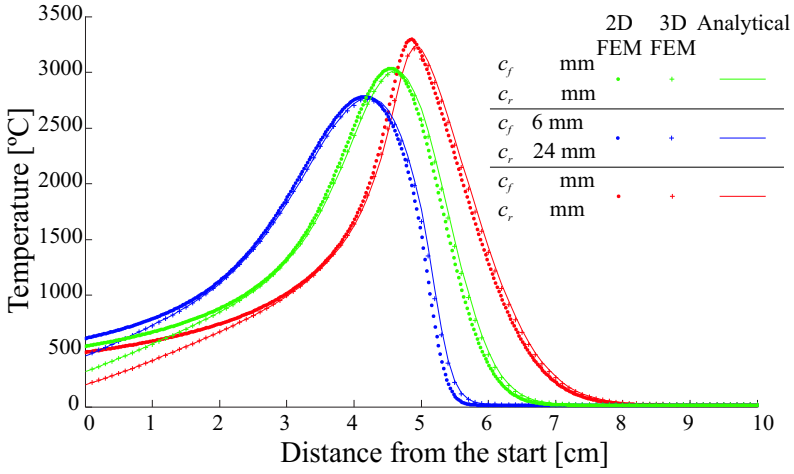

Figure 6: Analytical vs. FEM solutions for the temperature profile along the welding path 10 sec after the start of welding.

5 CONCLUSIONS

This work proposed an analytical solution for the unsteady heat conduction induced by a double-ellipsoidal moving heat source on a semi-infinite medium. This problem is of industrial interest since it is is representative of a wide variety of welding processes on thick plates.

The availability of an analytical solution enables the evaluation of a numerical solution free of experimental uncertainties. By using a quite fine spatial and time discretization, we obtained accurate results with linear tetrahedral finite elements for the whole 3D domain, while results using linear triangular finite elements for a cross section were satisfactory except for the run-on of the process. On the other hand, the computational consumption with the 2D model was two orders of magnitude lower than that required for the 3D model. This made the 2D model the

most convenient tool for the analysis of welding in regions far enough from the starting point.

ACKNOWLEDGEMENTS

We acknowledge support from European Community, contract AST 5-CT 2006-030953, project RAPOLAC (Rapid Production of Large Aerospace Components), CONICET (Consejo Nacional de Investigaciones Científicas y Técnicas, Argentina), and UNL (Universidad Nacional del Litoral, Argentina).

REFERENCES

Abid M. and Siddique M. Numerical simulation to study the effect of tack welds and root gap on welding deformations and residual stresses of a pipe-flange joint. *International Journal of Pressure Vessels and Piping*, 82:860–871, 2005.

Abid M., Siddique M., and Mufti R.A. Prediction of welding distortions and residual stresses in a pipe-flange joint using the finite element technique. *Modelling Simul. Mater. Sci. Eng.*, 13:455–470, 2005.

Bang I.W., Son Y.P., Oh K.H., Kim Y.P., and Kim W.S. Numerical simulation of sleeve repair welding of in-service gas pipelines. *Welding Journal*, pages 273–282, 2002.

Branza T., Duchosal A., Fras G., Deschaux-Beaume F., and Lours P. Experimental and numerical investigation of the weld repair of superplastic forming dies. *Journal of Materials Processing Technology*, 155–156:1673–1680, 2004.

Carslaw H.S. and Jaeger J.C. *Conduction of heat in solids*. Oxford University Press, second edition, 1959.

De A., Maiti S.K., Walsh C.A., and Badheshia H.K.D.H. Finite element simulation of laser spot welding. *Science and Technology of Welding and Joining*, 8(5):377–348, 2003.

Deng D. and Murakawa H. Numerical simulation of temperature field and residual stress in multi-pass welds in stainless steel pipe and comparison with experimental measurements. *Computational Materials Science*, 37:269–277, 2006a.

Deng D. and Murakawa H. Prediction of welding residual stress in multi-pass butt-welded modified 9Cr1Mo steel pipe considering phase transformation effects. *Computational Materials Science*, 37:209–219, 2006b.

Duranton P., Devaux J., Robin V., Gilles P., and Bergheau J.M. 3D modelling of multipass welding of a 316L stainless steel pipe. *Journal of Materials Processing Technology*, 153–154:457–463, 2004.

Gery D., Long H., and Maropoulos P. Effects of welding speed, energy input and heat source distribution on temperature variations in butt joint welding. *Journal of Materials Processing Technology*, 167:393–401, 2005.

Goldak J., Bibby M., Moore J., House R., and Patel B. Computer modelling of heat flow in welds. *Metallurgical Transactions B*, 17:587–600, 1986.

Goldak J., Chakravarti A., and Bibby M. A new finite element model for welding heat sources. *Metallurgical Transactions B*, 15:299–305, 1984.

Goldak J.A. and Akhlaghi M. *Computational Welding Mechanics*. Springer Science+Business Media, Inc., 2005.

Goldschmied G., Tschegg E.K., and Schuler A. Electron beam surface melting – numerical calculation of the melt geometry and comparison with experimental results. *J. Phys. D: Appl. Phys.*, 23:1686–1694, 1990.

Lei Y.C., Yu W.X., Li C.H., and Cheng X.N. Simulation on temperature field of TIG welding of copper without preheating. *Trans. Nonferrous Met. Soc. China*, 16:838–842, 2006.

Lundbäck A., Alberg H., and Henrikson P. Simulation and validation of TIG-welding and post weld heat treatment of an inconel 718 plate. In H. Cerjak, H.K.D.H. Bhadeshia, and E. Kozeschnik, editors, *Proceedings of the 7th International Seminar on the Numerical Analysis of Weldability*. Graz-Seggau, Austria, 2003.

Mendez P.F. *Joining Metals using Semi-Solid Slurries*. Master's thesis, Department of Materials Science and Engineering, Massachusetts Institute of Technology, 1995.

Nguyen N.T., Mai Y., Simpson S., and Ohta A. Analytical approximate solution for double ellipsoidal heat source in finite thick plate. *Welding Journal*, pages 82–93, 2004.

Nguyen N.T., Ohta A., Matsuoka K., Suzuki N., and Maeda Y. Analytical solutions for transient temperature of semi-infinite body subjected to 3-D moving heat sources. *Welding Research Supplement*, pages 265–274, 1999.

Open Engineering. OOFELIE::Multiphysics. 2008.

Reutzel E.W., Nelly S.M., Martukanitz R.P., Bugarewicz M.M., and Michaleris P. Laser-GMA hybrid welding: process monitoring and thermal modeling. In *Procs. of the 7th International Conference Trends in Welding Research*. Pine Mountain (USA), 2005.

Song J., Peters J., Noor A., and Michaleris P. Sensitivity analysis of the thermomechanical response of welded joints. *International Journal of Solids and Structures*, 40:4167–4180, 2003.

Thiessen R.G., Richardson I.M., and Sietsma J. Physically based modelling of phase transformations during welding of low-carbon steel. *Materials Science and Engineering A*, 427:223–231, 2006.

Wu C.S., Chen J., and Zhang Y.M. Numerical analysis of both front- and back-side deformation of fully-penetrated GTAW weld pool surfaces. *Computational Materials Science*, 39(3):635–642, 2007.

Wu C.S. and Yan F. Numerical simulation of transient development and diminution of weld pool in gas tungsten arc welding. *Modelling Simul. Mater. Sci. Eng.*, 12:13–20, 2006.